Journal of Alloys and Compounds 400 (2005) 56–61

Journal of ALLOYS AND COMPOUNDS

www.elsevier.com/locate/jallcom

Bulk modulus of CeO_2 and PrO_2—An experimental and theoretical study

L. Gerward [a,*], J. Staun Olsen [b], L. Petit [c,e], G. Vaitheeswaran [d], V. Kanchana [d], A. Svane [e]

[a] Department of Physics, Technical University of Denmark, Fysikvej 307, DK-2800 Kongens Lyngby, Denmark
[b] Niels Bohr Institute, Oersted Laboratory, University of Copenhagen, DK–2100 Copenhagen, Denmark
[c] Computational Science and Mathematics Division, Center for Computational Sciences, Oak Ridge National Laboratory, Oak Ridge, TN 37831-6114, USA
[d] Max-Planck-Institut für Festkörperforschung, Heisenbergstrasse 1, D–70569 Stuttgart, Germany
[e] Department of Physics and Astronomy, University of Aarhus, DK-8000 Aarhus C, Denmark

Received 2 March 2005; accepted 7 April 2005
Available online 23 May 2005

Abstract

The high-pressure structural behaviour of CeO_2 and PrO_2 has been investigated by synchrotron X-ray diffraction at pressures up to 20 and 35 GPa, respectively. The experiments are accompanied by first principles calculations using the self-interaction corrected local spin density (SIC-LSD) approximation. The experimental values for the zero-pressure bulk modulus of CeO_2 and PrO_2 are 220(9) and 187(8) GPa, respectively. Our calculations reproduce the lattice constants with good accuracy, but find identical bulk modulii for CeO_2 (176.9 GPa) and PrO_2 (176.8 GPa).
© 2005 Elsevier B.V. All rights reserved.

Keywords: X-ray diffraction; Crystal binding and equation of state; Electron band calculation; Synchrotron radiation; High pressure

1. Introduction

Lanthanide dioxides, which have a cubic fluorite structure, form an interesting and extensively studied series, which finds potential interest as optical component materials and laser hosts. The Ce, Pr and Tb dioxides crystallize in the cubic fluorite structure whereas the other rare earths form sesquioxides. CeO_2, commonly known as Ceria, has broad applications in industry and hence it has been most extensively studied by experimentalists as well as theoreticians. Bulk CeO_2 has got a wide range of application in modern catalytic industry [1,2]. In addition, the ability of CeO_2 to conduct oxygen ions has made it one of the basic materials for fuel-cell technologies [3]. PrO_2 is an insulator exhibiting type-I antiferromagnetic ordering below the Néel temperature $T_N = 14$ K with an anomalously low ordered moment of $0.6\mu_B$ [4], where μ_B is the Bohr magneton. PrO_2 forms high quality epitaxial films when grown on a hydrogen-terminated Si(1 1 1) surface [5].

Several experimental studies such as inelastic neutron scattering and neutron diffraction measurements on PrO_2 reveal evidence for Jahn–Teller distortion at $T_D = 120 \pm 2$ K [6,7]. Below this temperature an internal distortion of the oxygen sublattice causes the unit cell of the crystallographic structure to be doubled along one crystal axis [8,9]. Apart from neutron diffraction measurements, spectroscopic studies such as core-level photoemission, optical reflectivity, and fluorescence spectroscopy have been carried out for PrO_2 by several experimental groups [10–13].

Studies of CeO_2 and PrO_2 under pressure are interesting because they can be related to the systematics of the high-pressure behaviour of the lanthanide and actinide dioxides. Most cubic fluorite-type compounds (space group $Fm\bar{3}m$ (2 2 5)), such as CeO_2 and PrO_2, have been shown to transform to the orthorhombic $\alpha PbCl_2$-type structure (space group *Pnma* (62)) at high pressure. A key question in the theoretical description of CeO_2 and PrO_2 is the nature of the bonding and the occupation of the 4f orbital. One reason for the limited

* Corresponding author. Tel.: +45 45 25 31 46; fax: +45 45 93 2399.
E-mail address: gerward@fysik.dtu.dk (L. Gerward).

0925-8388/$ – see front matter © 2005 Elsevier B.V. All rights reserved.
doi:10.1016/j.jallcom.2005.04.008

number of theoretical studies could be the difficulty to describe the 4f electron state within standard band–structure methods.

High-pressure Raman studies on CeO_2 in comparison with the isostructural actinide dioxide ThO_2 indicate a pressure-induced phase transition from the fluorite phase around 31 GPa in CeO_2 and around 30 GPa in ThO_2 [14,15]. The high-pressure spectra are consistent with the lower-symmetry $\alpha PbCl_2$-type structure. These results were confirmed in the high-pressure X-ray diffraction studies of CeO_2 [16,17]. In both these studies, the bulk modulus of the fluorite-type phase was determined. The sound wave velocity for each acoustic phonon mode of CeO_2 was estimated by Nakajima et al. [18] from the frequency shift of Brillouin scattering lines. Using these experimental values, the elastic constants of CeO_2 were derived. Size-dependent properties of CeO_2 nanoparticles have been recently studied experimentally [19–22] using Raman spectroscopy and X-ray diffraction.

The presence of covalent bonding in CeO_2 and PrO_2 was demonstrated by Koelling et al. [23], by means of the linear augmented plane wave method. Hill and Catlow [24], in a study of bulk CeO_2, applied the restricted Hartree–Fock method to study the ground state properties. The computed bulk modulus was 357 GPa, which is about 50% larger than the experimental value. Later, Landrum et al. [25] carried out a systematic examination of the electronic structure and bonding in CeO_2 and other cerium compounds using the linear muffin–tin orbital (LMTO) method in the atomic sphere approximation.

Recently, electronic, bonding and optical properties of CeO_2 and Ce_2O_3 were calculated in the framework of the full-potential LMTO method, using the local-density approximation (LSDA) and the generalized gradient approximation (GGA) for the exchange-correlation potential [26]. It was found that the lattice parameter and the bulk modulus of CeO_2 estimated for a valence band model (treating the f electrons as valence states) are in much better agreement with experiment than those calculated for a core state model (treating the f electrons as core states). The best agreement between theory and experiment is obtained within the LSDA, whereas GGA calculations predict somewhat too large lattice constants and too small bulk modulii [26]. The mechanism behind the ability of ceria to store oxygen has been explained on the basis of first-principles quantum mechanical simulations by the same authors [27]. They further extended their study on the surface properties of CeO_2 from first principles [28].

Combined experimental and theoretical studies of the optical properties of CeO_2 along with other tetravalent Ce^{4+} ions confirmed the applicability of CeO_2 as a potential UV absorber [29]. Recently, Yang et al. [30] have studied the ground-state electronic properties of stoichiometric bulk as well as surfaces of reduced and unreduced CeO_2 using the Vienna ab initio simulation package. The projector-augmented wave method was used and shown to give a good description of the properties of bulk CeO_2. The results also show clearly that CeO_2 is an insulator.

Very little has been published on the high-pressure behaviour of PrO_2. High-pressure phase transformations of PrO_2 and some other isostructural fluorite-type dioxides have been studied using the diamond-anvil cell and laser heating. In PrO_2, a pressure induced structural phase transition from cubic fluorite phase to an orthorhombic phase similar to that of ThO_2 has been observed [31]. X-ray absorption studies of PrO_2 at pressures up to 12 GPa were carried out by Hu et al. [32]. Theoretically, calculations have been performed by Dabrowski et al. [33] to study the ground state properties of PrO_2 in the fluorite-type phase using an ab initio pseudopotential plane wave code, extended for atoms with valence electrons of f-type. The LSD method for the exchange and correlation energy and non-local pseudopotentials was used. The computed bulk modulus is 250 GPa, which is about 15% larger than the experimental value [33].

The present work is an experimental and theoretical study of the high-pressure structural behaviour of CeO_2 and PrO_2. In particular, we emphasize the determination of the equation of state and the bulk modulus of the cubic fluorite-type phase.

2. Experimental procedure

High-pressure powder X-ray diffraction patterns were recorded at room temperature using the white-beam method and synchrotron radiation at Station F3 of HASYLAB-DESY in Hamburg, Germany. The diffractometer, working in the energy-dispersive mode, has been described elsewhere [34]. High pressures were obtained in a Syassen–Holzapfel type diamond-anvil cell. A finely ground powder sample and a ruby chip were placed in a 200 μm diameter hole in an inconel gasket, pre-indented to a thickness of 60 μm. A 16:3:1 methanol:ethanol:water mixture was used as the pressure-transmitting medium. The pressure in the cell was determined from the wavelength shift of the ruby R_1 luminescence line and applying the non-linear pressure scale of Mao et al. [35]. The Bragg angle of each run was calculated from a zero-pressure spectrum of sodium chloride in the diamond-anvil cell.

Fig. 1 shows synchrotron X-ray diffraction diagrams for CeO_2 and PrO_2. From the observed diffraction pattern, values for the lattice parameter and the unit-cell volume as a function of pressure can be derived and refined. The pressure–volume data can then be described by an appropriate equation of state (EOS). In the present work, we have used the Birch–Murnaghan equation [36], which for a cubic phase can be written:

$$P = \frac{3}{2}B_0(x^{-7} - x^{-5})\left[1 - \frac{3}{4}(4 - B_0')(x^{-2} - 1)\right] \quad (1)$$

where $x = a/a_0$, a being the lattice parameter at pressure P, and a_0 the lattice parameter at zero pressure, B_0 is the bulk modulus and B_0' its pressure derivative, both parameters evaluated

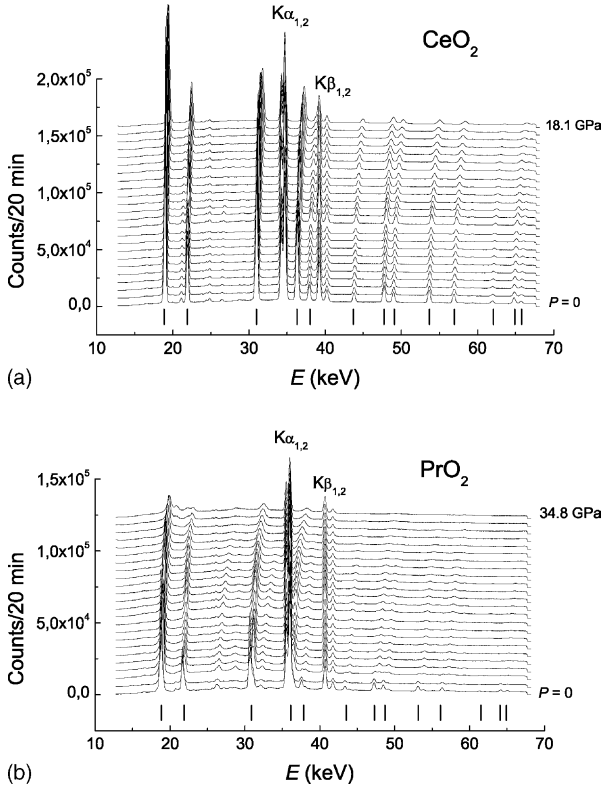

Fig. 1. Synchrotron X-ray diffraction spectrum at various pressures. The small vertical lines at the bottom of the diagram indicate the positions of the fluorite-phase Bragg-reflections: (a) CeO_2; (b) PrO_2.

at zero pressure. Values of B_0 and B_0' are obtained from a least-squares fit of Eq. (1) to the experimental data points.

3. Theoretical aspects

While the conventional band theory, as implemented in the local spin-density approximation to the density functional theory, generally has been very successful in describing solid state properties, it fails for f-electron systems. The strong on-site correlation effects that tend to localize the f-electrons in atomic-like orbitals are inadequately accounted for by the homogeneous electron gas underpinning the LSD. In fact, the LSD approximation introduces an unphysical self-interaction, which, though it vanishes for extended states in a periodic solid, can be substantial for well-localized states.

The self-interaction corrected (SIC)-LSD approximation constitutes a scheme capable of treating both localized and delocalized electrons on an equal footing, by including into the total energy functional an explicit energy contribution for an electron to localize [37]. The localized f-states thus gain the self-interaction energy, but loose their band formation energy, as they are no longer allowed to hybridize with the remaining conduction electrons. On balance, comparing different localized f^n scenarios, the global energy minimum establishes the ground state configuration. The details of the SIC-LSD method can be found in Ref. [38].

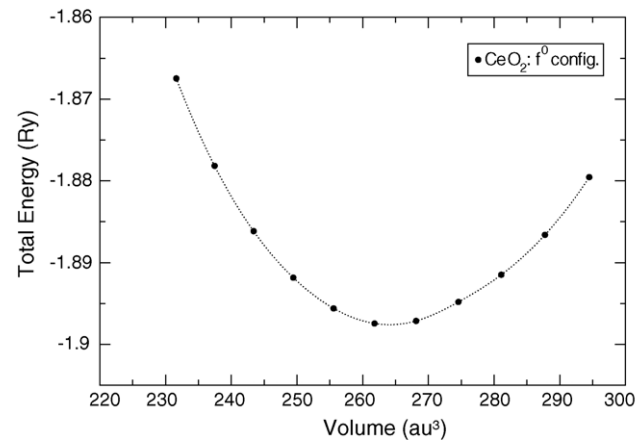

Fig. 2. Total energy as a function of volume for CeO_2 in the f^0 configuration.

Due to the highly correlated 4f electrons, the rare-earth compounds are characterized by a fixed f^n configuration of atomic-like f-electrons, and the resulting electronic structure is well reproduced within the SIC-LSD (see for example [39] and references therein). Calculations based on the LSD approximation indicate that the experimental observations are best reproduced by describing CeO_2 in terms of delocalized f-electrons and PrO_2 with one f-electron treated as core state. However, rather than determining the f-electron configuration from a comparison to empirical data, the SIC-LSD method is entirely ab initio, and relies on total energy calculations. Thus, comparing the total energies for various f-localization scenarios, the $Ce(f^0)$ and $Pr(f^1)$ configurations were found to be energetically most favourable [40]. The lattice constant and the bulk modulus for the given configuration can be derived from the total energy versus volume behaviour (depicted for the CeO_2 ground state configuration in Fig. 2) using the Birch–Murnaghan equation of state [36].

4. Results and discussion

Fig. 3a shows the experimental and theoretical lattice parameters of cubic CeO_2 as functions of pressure. A fit of the Birch–Murnaghan equation (1) to the experimental data points gives the zero-pressure bulk modulus $B_0 = 220(9)$ GPa and $B_0' = 4.4(4)$. Also shown in Fig. 3 is the compression curve calculated by the SIC-LSD method. The predicted zero-pressure lattice parameter $a_0 = 5.384$ Å agrees within 0.5% with the corresponding experimental value 5.411(1) Å. However, the SIC-LSD method seems to considerably underestimate the bulk modulus, the calculated B_0-value being 176.9 GPa, which is 20% lower than the experimental value.

Similarly, the lattice parameters of cubic PrO_2 as functions of pressure is shown in Fig. 3b. A fit of the Birch–Murnaghan equation (1) to the experimental data points gives $B_0 = 187(8)$ GPa and $B_0' = 4.8(5)$. Also here, the compression curve has been calculated by the SIC-LSD method.

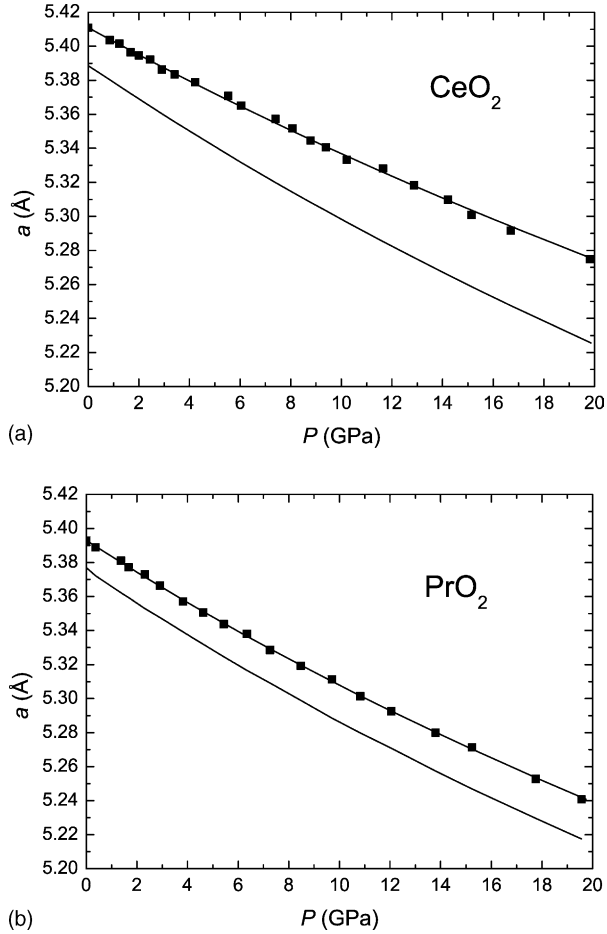

Fig. 3. Room-temperature compression curves. The curve through the experimental data points (filled squares) has been calculated from the Birch–Murnaghan equation (1). The result of the theoretical calculation is shown by the lower curve: (a) CeO_2; (b) PrO_2.

Again, the predicted zero-pressure lattice parameter 5.364 Å agrees with the corresponding experimental value 5.394(2) Å within 0.5%, whereas the calculated zero-pressure bulk modulus 176.8 GPa is 8% lower than the experimental value.

In Tables 1 and 2 we summarize experimental and calculated values of the zero-pressure lattice constant, a_0, and bulk modulus, B_0, for cubic CeO_2 and PrO_2 as obtained in the present work and as found in the literature. It is seen that the experimental values for the bulk modulus of CeO_2 (Table 1) are confined to a 15% range from 204 to 236 GPa, whereas there is a large scatter of the calculated values. Apart from the very high value of Hill and Catlow [24], calculations tend to underestimate the bulk modulus. For PrO_2 (Table 2) there are too few data to draw any general conclusions.

In Fig. 4a and b we show the ground state density of states (DOS) of CeO_2 and PrO_2, respectively. We notice that both DOSs are remarkably similar. Below the Fermi level,

Table 1
Comparison of experimental and calculated values of the lattice parameter a_0 and the zero-pressure bulk modulus B_0 of CeO_2

a_0 (Å)	B_0 (GPa)	Method	Reference
5.406(10)	230(10)	X-ray diffraction	[16]
5.411(3)	236(4)	X-ray diffraction	[17]
	204	Brillouin scattering	[18]
5.385	357	Hartree–Fock	[24]
5.39	215	FP-LMTO	[26]
5.45	194	VASP-PAW	[30]
5.411(1)	220(9)	X-ray diffraction	Present work
5.384	176.9	SIC-LSD	Present work

The number in parentheses is in each case the estimated error or the standard error of the fit, in units of the last decimal place.

Table 2
Comparison of experimental and calculated values of the lattice parameter a_0 and the zero-pressure bulk modulus B_0 of PrO_2

a_0 (Å)	B_0 (GPa)	Method	Reference
	250	LSD	[33]
5.394(2)	187(8)	X-ray diffraction	Present work
5.364	176.8	SIC-LSD	Present work

The number in parentheses is in each case the estimated error or the standard error of the fit, in units of the last decimal place.

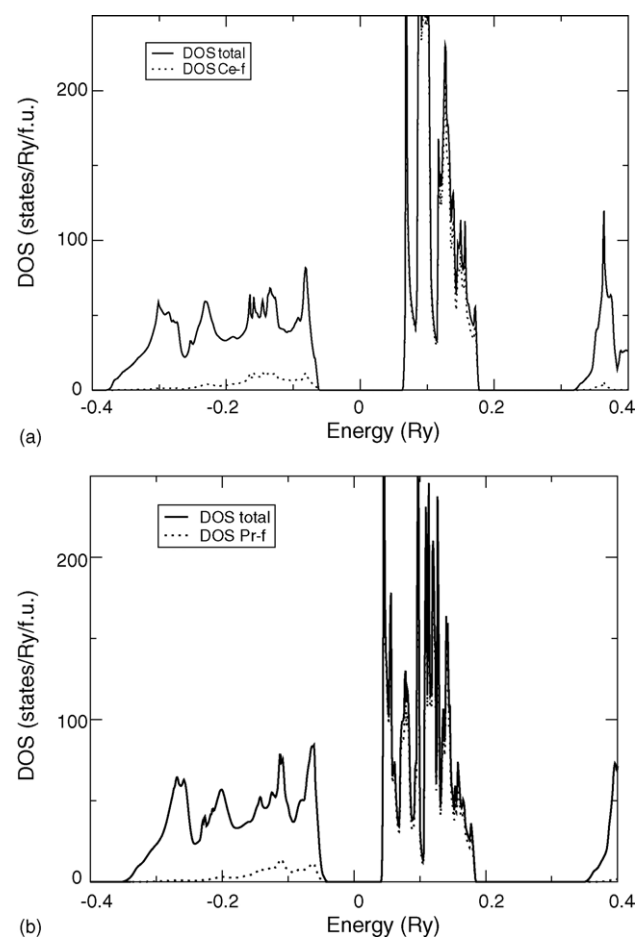

Fig. 4. DOS plots: (a) CeO_2 in the f^0 configuration; (b) PrO_2 in the f^1 configuration.

the oxygen *p* band is completely filled by accommodating two electrons from the rare earth element through charge transfer and hybridization. Above the Fermi level we find the unoccupied f-levels. In a pure LSD picture, the additional f-electron of Pr would be placed in the narrow band state above the energy gap, resulting in a large DOS at the Fermi level, which is in disagreement with the insulating nature of PrO_2. Here, in the SIC-LSD, we find that the f-electron prefers to occupy an atomic like orbital due to the associated gain in self-interaction energy. The ground state DOS for CeO_2 in Fig. 4a is obtained from the LSD approximation. The calculated energy gaps are 1.7 eV for CeO_2 and 1.1 eV for PrO_2, respectively. The experimental BIS spectrum shows a minimum energy gap of around 3 eV for CeO_2 [41], and conductivity measurements indicate a gap of 0.26 eV for PrO_2 [42]. Given the considerable similarity between the two DOSs, it may not be surprising that the calculated bulk modulii are more or less the same for the two compounds. This cannot, however, explain the large difference of about 15% between the actually measured values for CeO_2 and PrO_2.

In summary, the experimental zero-pressure bulk modulii for cubic fluorite-type CeO_2 and PrO_2, as determined in the present work, are 220(9) and 187(8) GPa, respectively. Calculations using the self-interaction corrected local-density approximation reproduce the insulating nature of CeO_2 and PrO_2 compounds and the measured equilibrium lattice constants within 0.5%. The calculated bulk modulii are found to be almost equal for the two compounds and 20% and 8%, respectively, lower than the measured value. This discrepancy could be due to limitations of the present LMTO-ASA implementation.

Acknowledgements

We thank HASYLAB-DESY for permission to use the synchrotron radiation facility. Part of this work was supported by the European Community, Research Infrastructure Action under the FP6 Structuring the European Research Area Programme (through the Integrated Infrastructure Initiative Integrating Activity on Synchrotron and Free-Electron Laser Science). L.G. and J.S.O. acknowledge financial support from the Danish Natural Science Research Council through DANSYNC. V.K. and G.V. acknowledge the Max-Planck Society for financial support. The work of L.P. is supported in part by Defence Advanced Research Project Agency and by the Division of Materials Science and Engineering, US Department of Energy, under contract no. DE-AC05-000R22725 with UT-Battelle LLC.

References

[1] A. Trovarelli, Catal. Rev. Sci. Eng. 38 (1996) 439.
[2] A. Trovarelli, Catalysis by Ceria and Related Materials, Imperial College Press, 2002.
[3] M.S. Dresselhaus, I.L. Thomas, Nature (London) 414 (2001) 332.
[4] S. Kern, C.-K. Loong, J. Faber Jr., G.H. Lander, Solid State Commun. 49 (1984) 295.
[5] D.K. Fork, D.B. Fenner, T.H. Geballe, J. Appl. Phys. 68 (1990) 4316.
[6] A.T. Boothroyd, C.H. Gardiner, S.J.S. Lister, P. Santini, B.D. Rainford, L.D. Noailles, D.B. Currie, R.S. Eccleston, R.I. Bewley, Phys. Rev. Lett. 86 (2001) 2082.
[7] C.H. Gardiner, A.T. Boothroyd, P. Pattison, M.J. McKelvy, G.J. McIntyre, S.J.S. Lister, Phys. Rev. B 70 (2004) 024415.
[8] C.H. Gardiner, A.T. Boothroyd, S.J.S. Lister, M.J. Mckelvy, S. Hull, B.H. Larsen, Appl. Phys. A 74 (2002) 1773.
[9] T. Lancaster, S.J. Blundell, F.L. Pratt, C.H. Gardiner, W. Hayes, A.T. Boothroyd, J. Phys. Condens. Matter 15 (2003) 8407.
[10] A. Bianconi, A. Kotani, K. Okada, R. Giorgi, A. Gargano, A. Marcelli, Phys. Rev. B 38 (1988) 3433.
[11] A. Bianconi, T. Miyahara, A. Kotani, Y. Kitajima, T. Yokoyama, H. Kuroda, M. Funabashi, H. Arai, T. Ohta, Phys. Rev. B 39 (1989) 3380.
[12] S. Kimura, F. Arai, M. Ikezawa, J. Electron Spectrosc. Relat. Phenom. 78 (1996) 135.
[13] S.M. Butorin, L.-C. Duda, J.-H. Guo, N. Wassadahl, J. Nordgren, M. Nakazawa, A. Kotani, J. Phys. Condens. Matter 9 (1997) 8155.
[14] G.A. Kourouklis, A. Jayaraman, G.P. Espinosa, Phys. Rev. B 37 (1988) 4250.
[15] A. Jayaraman, G.A. Kourouklis, L.G. Van Uitert, Pramana J. Phys. 30 (1988) 225.
[16] S.J. Duclos, Y.K. Vohra, A.L. Ruoff, A. Jayaraman, G.P. Espinosa, Phys. Rev. B 38 (1988) 7755.
[17] L. Gerward, J.S. Olsen, Powder Diffr. 8 (1993) 127.
[18] A. Nakajima, A. Yoshihara, M. Ishigama, Phys. Rev. B 50 (1994) 13297.
[19] J.E. Spanier, R.D. Robinson, F. Zhang, S.-W. Chan, I.P. Herman, Phys. Rev. B 64 (2001) 245407.
[20] S. Rekhi, S.K. Saxena, P. Lazor, J. Appl. Phys. 89 (2001) 2968.
[21] Z. Wang, S.K. Saxena, V. Pischedda, H.P. Liermann, C.S. Zha, Phys. Rev. B 64 (2001) 012102.
[22] Z. Wang, Y. Zhao, D. Schiferl, C.S. Zha, R.T. Downs, Appl. Phys. Lett. 85 (2004) 124.
[23] D.D. Koelling, A.M. Boring, J.H. Wood, Solid State Commun. 47 (1983) 227.
[24] S.E. Hill, C.R.A. Catlow, J. Phys. Chem. Solids 54 (1993) 411.
[25] G.A. Landrum, R. Dronskowski, R. Niewa, F.J. DiSalvo, Chem. Eur. J. 5 (1999) 515.
[26] N.V. Skorodumova, R. Ahuja, S.I. Simak, I.A. Abrikosov, B. Johansson, B.I. Lundqvist, Phys. Rev. B 64 (2001) 115108.
[27] N.V. Skorodumova, S.I. Simak, B.I. Lundqvist, I.A. Abrikosov, B. Johansson, Phys. Rev. Lett. 89 (2002) 166601.
[28] N.V. Skorodumova, M. Baudin, K. Hermansson, Phys. Rev. B 69 (2004) 075401.
[29] F. Goubin, X. Racquefelte, M-H. Whangbo, Y. Montardi, R. Brec, S. Jobic, Chem. Mater. 16 (2004) 662.
[30] Z. Yang, T.K. Woo, M. Baudin, K. Hermansson, J. Chem. Phys. 120 (2004) 7741.
[31] L.-G. Liu, Earth Planet. Sci. Lett. 49 (1980) 166.
[32] Z. Hu, S. Bertram, G. Kaindl, Phys. Rev. B 49 (1994) 39.
[33] J. Dabrowski, V. Zavodinsky, A. Fleszar, Microelectron. Reliab. 41 (2001) 1093.
[34] J.S. Olsen, Rev. Sci. Instrum. 83 (1992) 1058.
[35] H.K. Mao, J. Xu, P.M. Bell, J. Geophys. Res. 91 (1986) 4673.
[36] F.J. Birch, J. Appl. Phys. 9 (1938) 279;
F.J. Birch, Phys. Rev. 71 (1947) 809.
[37] J.P. Perdew, A. Zunger, Phys. Rev. B 23 (1981) 5048.

[38] A. Svane, Phys. Rev. B 53 (1996) 4275.
[39] A. Svane, P. Strange, W.M. Temmerman, Z. Szotek, H. Winter, L. Petit, Phys. Stat. Sol. (b) 223 (2001) 105.
[40] L. Petit, A. Svane, Z. Szotek, W.M. Temmerman, submitted for publication.
[41] E. Wuilloud, B. Delley, W.-D. Schneider, Y. Baer, Phys. Rev. Lett. 53 (1984) 202.
[42] G.H. Gardiner, A.T. Boothroyd, P. Pattison, M.J. McKelvy, G.J. McIntyre, S.J.S. Lister, Phys. Rev. B 70 (2004) 024415.